

# Physically based assessment of hurricane surge threat under climate change

Ning Lin<sup>1\*</sup>, Kerry Emanuel<sup>1</sup>, Michael Oppenheimer<sup>2</sup> and Erik Vanmarcke<sup>3</sup>

**Storm surges are responsible for much of the damage and loss of life associated with landfalling hurricanes. Understanding how global warming will affect hurricane surges thus holds great interest. As general circulation models (GCMs) cannot simulate hurricane surges directly, we couple a GCM-driven hurricane model with hydrodynamic models to simulate large numbers of synthetic surge events under projected climates and assess surge threat, as an example, for New York City (NYC). Struck by many intense hurricanes in recorded history and prehistory, NYC is highly vulnerable to storm surges. We show that the change of storm climatology will probably increase the surge risk for NYC; results based on two GCMs show the distribution of surge levels shifting to higher values by a magnitude comparable to the projected sea-level rise (SLR). The combined effects of storm climatology change and a 1 m SLR may cause the present NYC 100-yr surge flooding to occur every 3–20 yr and the present 500-yr flooding to occur every 25–240 yr by the end of the century.**

Associated with extreme winds, rainfall and storm surges, tropical cyclones present major hazards for coastal areas. Moreover, tropical cyclones respond to climate change<sup>1–3</sup>. Previous studies predicted an increase in the global mean of the maximum winds and rainfall rates of tropical cyclones in a warmer climate<sup>4</sup>; however, the effect of climate change on storm surges, the most damaging aspect of tropical cyclones, remains to be investigated<sup>4</sup>. Hurricane Katrina of 2005, the costliest natural disaster in US history, produced the greatest coastal flood heights ever recorded in the US, causing more than US\$100 billion in losses and resulting in about 2,000 fatalities. On the eastern US coast, where tropical cyclones are less frequent than in the Gulf of Mexico and Florida regions, the Great Hurricane of 1938 produced record flood heights in Long Island and southern New England, killing 600–800 people. A question of increasing concern is whether such devastating surge events will become more frequent.

The storm surge is a rise of coastal shallow water driven by a storm's surface wind and pressure gradient forces; its magnitude is determined, in a complex way, by the characteristics of the storm plus the geometry and bathymetry of the coast. As a result, the change of surge severity cannot be inferred directly from the change of storm intensity<sup>5–8</sup>. For example, Hurricane Camille of 1969 (category 5) made landfall in the same region of Mississippi as the less intense Hurricane Katrina (category 3), but produced lower surges owing to its smaller size<sup>5,6,9</sup>. Using only a storm's landfall characteristics to predict surges is also inaccurate<sup>10,11</sup>, as the evolution of the storm before and during landfall affects the surge. Furthermore, similar storms can produce quite different surges at locations with different topological features<sup>6</sup>. Therefore, quantifying the impact of climate change on hurricane surges requires explicit modelling of the development of storms and induced surges at regional scales under projected climates.

Modelling hurricane surges under climate scenarios, however, is not straightforward, because tropical cyclones cannot be resolved in present GCMs owing to their relatively low resolution (~100 km) when compared with the size of the storm core (~5 km). Although

high-resolution regional models (for example, refs 12 and 13) may be used to downscale the GCM simulations, these models are still limited in horizontal resolution and are too expensive to implement for risk assessment. This study takes a more practical approach, coupling a simpler GCM-driven statistical/deterministic hurricane model with hydrodynamic surge models to simulate cyclone surges for different climates.

Computationally efficient, this method can be used to generate large numbers of synthetic surge events at sites of interest, providing robust statistics to characterize surge climatology and extremes. We apply this method to investigate present and future hurricane surge threat for NYC, considering also the contribution of wave set-up, astronomical tides and SLR. The resulting surge flood return-level curves provide scientific bases for climate adaptation and sustainable development in rapidly developing coastal areas<sup>14–16</sup>.

## Storm simulation

The statistical/deterministic hurricane model<sup>17,18</sup> used in this study generates synthetic tropical cyclones under given large-scale atmospheric and ocean environments, which may be estimated from observations or climate modelling. This method does not rely on the limited historical track database, but rather generates synthetic storms that are in statistical agreement with observations<sup>17</sup>, and it compares well with various other methods used to study the effects of climate change on tropical cyclones<sup>4,18,19</sup>. In this study, we assume the cyclone-threatened area for NYC to be within a 200-km radius from the Battery (74.02 W, 40.9 N; chosen as the representative location for NYC), and we call it a NY-region storm if a storm ever passes within this area with a maximum wind speed greater than 20 m s<sup>-1</sup>. To investigate the present surge probabilities, we generate a set of 5,000 NY-region storms under the observed climate (represented by 1981–2000 statistics) estimated from the National Center for Environmental Prediction/National Center for Atmospheric Research (NCEP/NCAR) reanalysis<sup>20</sup>. To study the impact of climate change, we apply each of four climate models, CNRM-CM3 (Centre National de Recherches Météorologiques, Météo-France), ECHAM5 (Max Planck Institute), GFDL-CM2.0 (National Oceanic

<sup>1</sup>Department of Earth, Atmospheric, and Planetary Sciences, Massachusetts Institute of Technology, Cambridge, Massachusetts 02139-4307, USA,

<sup>2</sup>Department of Geosciences and the Woodrow Wilson School, Princeton University, Princeton, New Jersey 08544, USA, <sup>3</sup>Department of Civil and Environmental Engineering, Princeton University, Princeton, New Jersey 08544, USA. \*e-mail: ninglin@mit.edu.

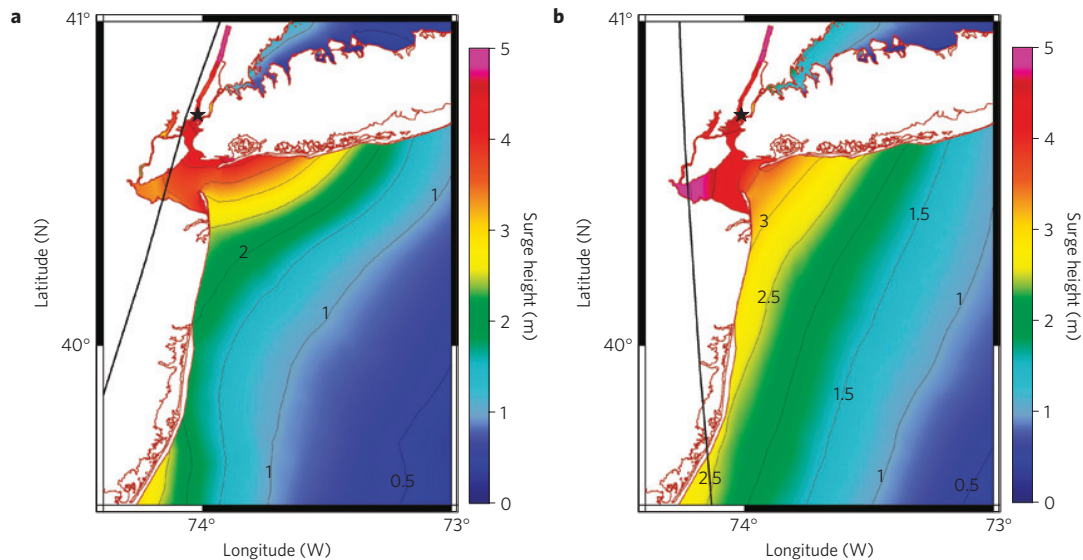


**Figure 1 | Two worst-case surge events for the Battery, under the NCEP/NCAR climate.** The contours and colours show the surge height (m). The black curve shows the storm track. The black star marks the location of the Battery. The storm parameters when the storm is closest to the Battery are as follows. **a**, Storm symmetrical maximum wind speed  $V_m = 56.6 \text{ m s}^{-1}$ , minimum sea-level pressure  $P_c = 960.1 \text{ mb}$ , radius of maximum wind  $R_m = 39.4 \text{ km}$ , translation speed  $U_t = 15.3 \text{ m s}^{-1}$  and distance to the site  $ds = 3.9 \text{ km}$ . **b**,  $V_m = 52.1 \text{ m s}^{-1}$ ,  $P_c = 969.2 \text{ mb}$ ,  $R_m = 58.9 \text{ km}$ ,  $U_t = 9.7 \text{ m s}^{-1}$  and  $ds = 21.1 \text{ km}$ .

and Atmospheric Administration (NOAA) Geophysical Fluid Dynamics Laboratory) and MIROC3.2 (CCSR/NIES/FRCGC, Japan), to generate 5,000 NY-region storms under present climate conditions (1981–2000 statistics) and another 5,000 NY-region storms under future climate conditions (2081–2100 statistics) for the A1B emission scenario of the Intergovernmental Panel on Climate Change (IPCC) fourth assessment report<sup>21</sup> (AR4). (Most of the climate data are obtained from the World Climate Research Program (WCRP) third Climate Model Intercomparison Project (CMIP3) multimodel data set.) We choose these four climate models because the predictions of the changes in storm frequency, intensity and power dissipation in the Atlantic basin due to global warming by these models span the range of predictions by all seven CMIP3 models from which the required model output is available<sup>18</sup>.

The annual frequency of the historical NY-region storms is estimated from the best-track Atlantic hurricane data set (updated from ref. 22) to be 0.34; we assume this number to be the storm annual frequency under the present climate. As the hurricane model does not produce an absolute rate of genesis, the storm frequency derived from each climate model for the present climate is calibrated to the observed value (0.34), and the frequency for the future climate is then predicted<sup>18</sup>. Estimated annual frequencies of future NY-region storms from the four climate models differ: CNRM is 0.70, ECHAM is 0.31, GFDL is 1.34 and MIROC is 0.29; the change of the storm frequency ranges from a decrease of 15% to an increase of 290%. The large variation among the model predictions reflects the general uncertainties in climate models' projections of tropical cyclone frequency, due to systematic model differences and internal climate variability (which may not be averaged out over the 20-yr periods considered here). According to ref. 23, as much as half of the uncertainty may be due to the climate variability. Moreover, the variations in the storm frequency changes at global or basin scales, as projected by refs 4 and 18, are greatly amplified at regional scales, owing to the differences in the changes of the storm track and intensity predicted by the climate models. We also note that even larger variations in the storm frequency changes can be induced if more climate models are considered; for example, the Hadley Center UK Meteorological Office model UKMO-HadCM3 may predict a relatively large reduction in the storm frequency due to climate change<sup>3</sup>.

### Surge modelling

This study uses two hydrodynamic models: the Advanced Circulation<sup>24,25</sup> (ADCIRC) model and the Sea, Lake, and Overland Surges from Hurricanes<sup>26</sup> (SLOSH) model, both of which have been validated and applied to simulate storm surges and make forecasts for various coastal regions (for example, refs 27–32). Storm surges are driven by storm surface wind and sea-level pressure fields. For the ADCIRC simulations, the surface wind is estimated by calculating the wind velocity at the gradient level with an analytical hurricane wind profile<sup>33</sup>, translating the gradient wind to the surface level with a velocity reduction factor (0.85; ref. 34) and an empirical expression of inflow angle<sup>35</sup>, and adding a fraction (0.5; based on observed statistics) of the storm translation velocity to account for the asymmetry of the wind field; the surface pressure is estimated from a parametric pressure model<sup>36</sup>. For the SLOSH simulations, the wind and pressure are determined within the SLOSH model by a semi-parametric hurricane model<sup>26</sup>. The two hydrodynamic models are applied with numerical grids of various resolutions (from  $\sim 1 \text{ km}$  to  $\sim 10 \text{ m}$  around NYC). The SLOSH simulation with a coarse-resolution grid is used to select the extreme surge events, which are further analysed with higher-resolution ADCIRC simulations to estimate the probability distributions of NYC surges (see Methods and Supplementary Figs S1 and S2).

As examples, Fig. 1 shows the spatial distribution of the storm surge around the NYC area for two worst-case scenarios for the Battery under the NCEP/NCAR climate. The storm that generates the highest surge (4.75 m) at the Battery moves northeastward and close to the site with a high intensity (Fig. 1a). A relatively weaker storm that moves farther from the site also produces a comparable surge (4.57 m) at the Battery, owing to its larger size and northwestward translation (Fig. 1b). Both storms induce high surges at the site with their largest wind forces to the right of the track, especially the northwestward-moving storm, which concentrates its strongest wind forces on pushing water into New York harbour and up to lower Manhattan. These two worst-case surges for the Battery have very low occurrence probabilities under the present climate condition. However, NYC has indeed been affected by numerous intense storm surges in recorded history and, on the basis of the local sedimentary evidence, prehistory<sup>37</sup>. The highest water level at the Battery as inferred from historic archives

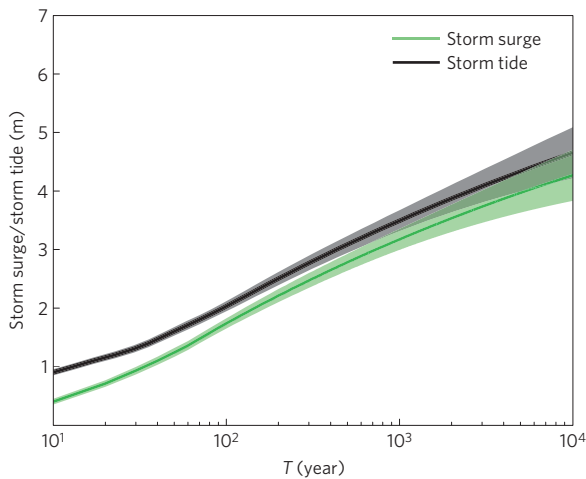


**Figure 2 | Estimated return levels for the Battery of the storm surge and storm tide for the NCEP/NCAR climate.** The shade shows the 90% confidence interval.

was about 3.2 m relative to the modern mean sea level, due to a hurricane in 1821 striking NYC at a low tide<sup>37</sup>; thus, the largest historical surge at the Battery might be about 3.8 m (given the magnitude of the local low tide of about 0.5–0.8 m).

We also investigate the influences of other processes related to the surge for NYC, using a set of over 200 most extreme surge events. To investigate the effects of wave set-up, we simulate the extreme events with the ADCIRC model coupled with a wave model<sup>32</sup>; the wave set-up is found to be small for the study region (see Supplementary Fig. S3), and thus it is neglected in our estimation of surge probabilities. We notice, however, that the nonlinear effect of the astronomical tide on the surge (tide-surge nonlinearity) is relatively large (see Supplementary Fig. S4). We model this nonlinearity as a function of the surge and tidal characteristics, based on a database generated for the extreme events (see Methods and Supplementary Fig. S5). This function is then used to estimate the storm tide as a combination of the surge and astronomical tide.

In addition, we study the nonlinear effect on the surge from the SLR, by simulating the extreme surges for a range of projected SLRs for NYC. This SLR effect is found to be negligible (see Supplementary Fig. S6), and thus the projected SLR in future climates is accounted for linearly in the estimation of the flood height for NYC.

### Statistical analysis

We assume the annual number of NY-region storms to be Poisson-distributed (Supplementary Fig. S7 and associated discussion), with the annual storm frequency as the mean. For each storm arrival, the probability density function (PDF) of the induced surge is estimated from the generated surge database. Our empirical data sets show that the surge PDF is characterized by a long tail, which determines the risk. We apply a peaks-over-threshold method to model this tail with a generalized Pareto distribution, using the maximum-likelihood method, and the rest of the distribution with non-parametric density estimation. The generalized Pareto distribution fits relatively well with the surge distribution for almost all storm sets in this study (Supplementary Figs S8 and S9). The estimated storm frequency and surge PDF are then combined to generate the surge return-level curve and associated statistical confidence interval (calculated with the Delta method<sup>38</sup>). The storm frequency and surge PDF are further applied to estimate the storm tide and flood height return levels (see Methods).

### Present surge threat

The estimated return levels of the storm surge at the Battery under the NCEP/NCAR climate are shown in Fig. 2. The estimated present 50-yr storm surge is about 1.24 m, the 100-yr surge is about 1.74 m and the 500-yr surge is about 2.78 m. A previous study<sup>39</sup>, using the SLOSH model with a relatively coarse mesh, predicted a higher surge (2.14 m) for the 100-yr return period but slightly lower surges for longer return periods for this site. These differences result mainly from the different wind profiles and grid resolutions applied in the ADCIRC and SLOSH simulations and the different storm sets (statistical samples) used. The estimated return level of the storm tide, shown also in Fig. 2, is about 0.3–0.5 m higher than the storm surge level. Thus, the estimated present 50-yr storm tide is about 1.61 m, the 100-yr storm tide is about 2.03 m and the 500-yr

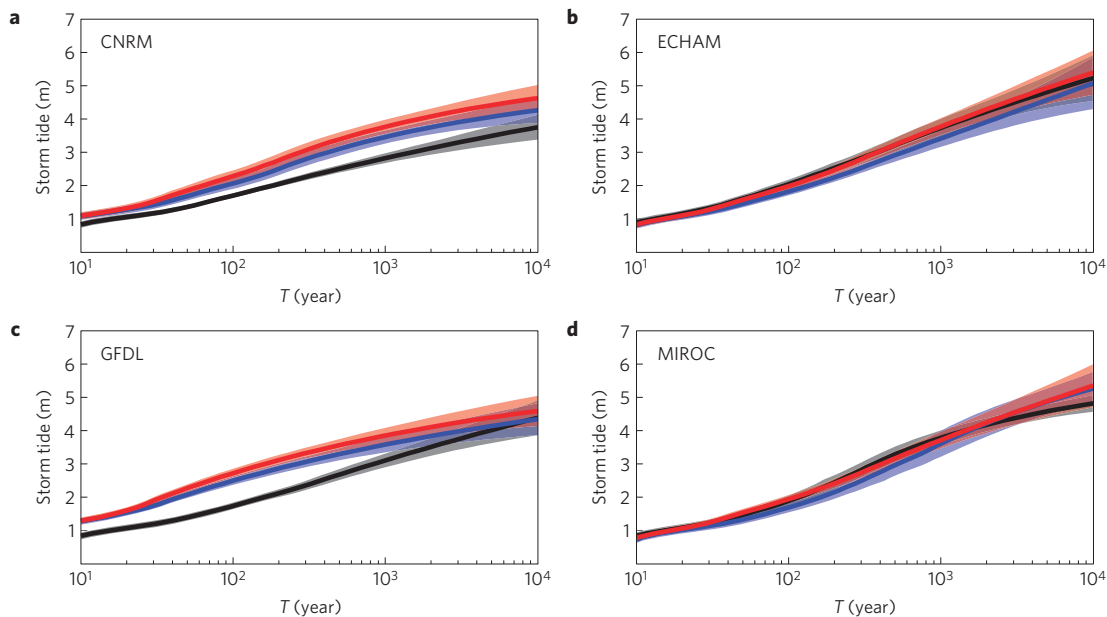


**Figure 3 | Estimated storm tide return levels for the Battery, predicted with each of the four climate models.** The black is for the present climate, the blue is for the IPCC A1B climate and the red is for the IPCC A1B climate with  $R_0$  increased by 10% and  $R_m$  increased by 21%. The shade shows the 90% confidence interval.

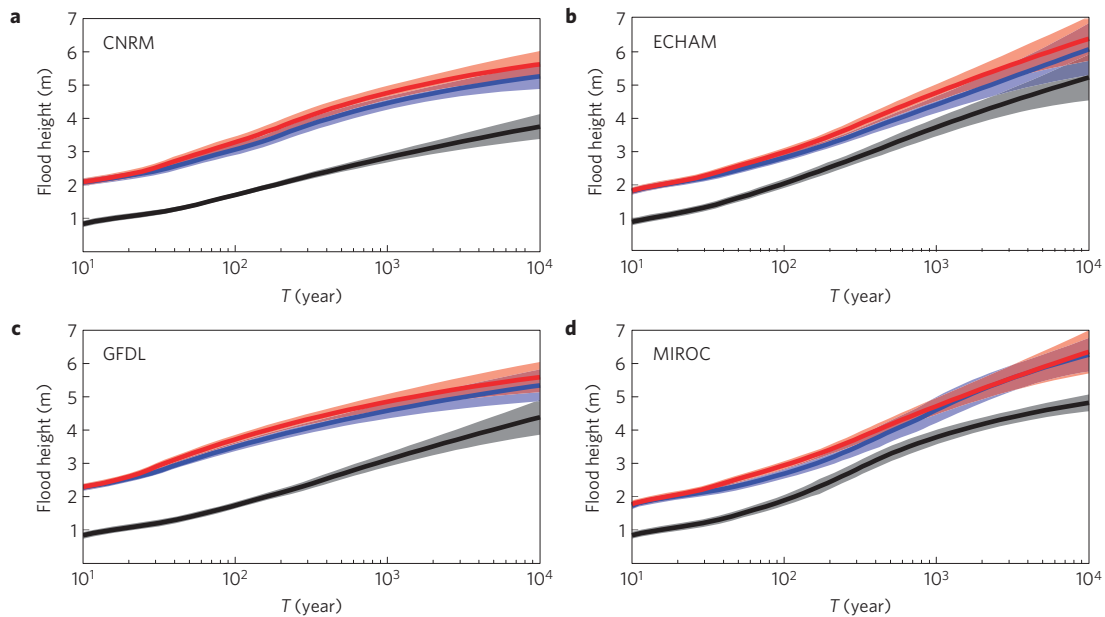


**Figure 4 | Estimated flood return levels for the Battery, predicted with each of the four climate models.** The black is for the present climate, the blue is for the IPCC A1B climate and the red is for the IPCC A1B climate with  $R_0$  increased by 10% and  $R_m$  increased by 21%. The shade shows the 90% confidence interval. The SLR for the A1B climate is assumed to be 1 m.

storm tide is about 3.12 m. Considering that much of the sea wall protecting lower Manhattan is only about 1.5 m above the mean sea level<sup>30</sup>, NYC is now highly vulnerable to extreme hurricane-surge flooding. For return periods under 50 yr, extratropical cyclones may also contribute to the coastal flooding risk and become the main source of 1–10 yr coastal floods for NYC<sup>40,41</sup>.

### Impact of climate change

The predictions of storm tide return levels for present and future IPCC A1B climates are presented in Fig. 3. (In the context of climate change, the return level at period  $T$  may be understood as the level with an annual exceedance probability of  $1/T$ .) The results from the four climate models differ: CNRM predicts an increase of the storm tide level, whereas ECHAM predicts a decrease; GFDL predicts that the storm tide level will increase for the main range of the return period but decrease for very long return periods, whereas MIROC predicts a decrease for low and moderate return periods but an increase for longer return periods. However, the magnitudes of the change (the ratio of A1B to the present-climate level) using CNRM (1.13–1.24) and GFDL (0.98–1.44) are more significant than those using ECHAM (0.89–0.96) and MIROC (0.89–1.08). The discrepancies among the model results can be attributed to the models' different estimations of the change of the storm frequency and the surge severity. The storm frequency at a regional scale plays an important role in determining the surge risk; the prediction of the frequency change for NY-region storms by the four climate models varies greatly. Moreover, unlike the average storm intensity, which is predicted to increase by these and other climate models<sup>4</sup>, the storm surge severity is predicted to increase by some models but decrease by others. This difference is the result of the surge magnitude depending on the storm's intensity as well as other parameters, all of which may change differently in the different climate models.

We suspect that a main reason that the increase of storm intensity (in some models) does not translate to an increase in surge magnitude is that the storm's radius of maximum wind ( $R_m$ ) tends to decrease as the storm's intensity increases, given the assumption made in the above simulations that the distribution of the storm's outer radius ( $R_o$ , determined from observed statistics<sup>42</sup>) remains the same under different climates. However, in theory

the storm's overall dimension scales linearly with the potential intensity<sup>43</sup>; therefore, the increase of potential intensity in a warmer climate<sup>44</sup> may induce an increase of  $R_o$ . Consequently, the reduction of  $R_m$  due to the increase of storm intensity may be offset and even reversed. In such a case, climate change will probably increase storm intensity and size simultaneously, resulting in a significant intensification of storm surges. To test this hypothesis, we carry out the simulations as before but assume that  $R_o$  increases by 10% and  $R_m$  increases by 21% in the future climate. We base this assumption on the estimated change of the potential intensity (expected to increase by about 10%; ref. 4) and on a theoretical scaling relationship between  $R_o$  and  $R_m$  ( $R_m$  scales with  $R_o^2$ ; ref. 33). The storm tide level thus predicted, shown also in Fig. 3, is higher or nearly unchanged in the future climate for the four models. The magnitude of the change also grows owing to the increase of the storm size; it becomes 1.23–1.36 for CNRM, 1.05–1.50 for GFDL, 0.95–1.02 for ECHAM and 0.97–1.11 for MIROC. At present, the effect of climate change on hurricane size has yet to be investigated; therefore, it is uncertain whether the surge will greatly increase owing to the simultaneous increase in storm intensity and size or only moderately change when one factor increases while the other decreases. Further study of the storm size distribution under different climates is needed to answer this question.

### Discussion

As the climate warms, the global mean sea level is projected to rise, owing to thermal expansion and melting of land ice. Superimposed on the global SLR, regional sea levels may change owing to local land subsidence and ocean circulation changes, both of which are expected to significantly increase sea level in the NYC area<sup>45,46</sup>. The total SLR for NYC is projected to be in the range of 0.5–1.5 m by the end of the century<sup>21,40,47</sup>. The effect of SLR, rather than changes in storm characteristics, has been the focus of most studies on the impact of climate change on coastal flooding risk (for example, refs 45 and 48); some studies also account for the change of hurricane intensity due to the change of the sea surface temperature (for example, refs 49 and 50). To our knowledge, this paper is the first to explicitly simulate large numbers of hurricane surge events under projected climates to



assess surge probability distributions. Our study shows that some climate models predict the increase of the surge level due to the change of storm climatology to be comparable to the projected SLR for NYC. For example, the CNRM and GFDL models predict that, by the end of the century, the 100-yr and 500-yr storm tide levels will increase by about 0.7–1.2 m (Fig. 3a,c). More consequential, the combined effect of storm climatology change and SLR will greatly shorten the surge flooding return periods. As shown by the estimated flood return level in Fig. 4, if we assume the SLR in the NYC area to be 1 m, by the end of the century, the present NYC 100-yr surge flooding may occur every 20 yr or less (with CNRM, GFDL, ECHAM and MIROC yielding predictions of 4/4, 3/3, 21/20 and 14/13 yr, respectively, for observed/increased storm size) and the present 500-yr surge flooding may occur every 240 yr or less (with CNRM, GFDL, ECHAM and MIROC yielding predictions of 45/29, 28/24, 188/140 and 241/173 yr, respectively). These findings are dependent on the climate models used to generate the environmental conditions for the storm simulations, so other climate models may produce different results. Nevertheless, all four climate models used in this study predict significant increases in the surge flood level due to climate change, providing an additional rationale for a comprehensive approach to managing the risk of climate change, including long-term adaptation planning and greenhouse-gas emissions mitigation.

**Methods**

High-resolution surge simulations are computationally intensive; therefore, to make it possible to simulate surges with reasonable accuracy for the large synthetic storm sets, we apply the two hydrodynamic models with numerical grids of various resolutions in such a way that the main computational effort is concentrated on the storms that determine the risk of concern. First, the SLOSH simulation, using a polar grid with a resolution of about 1 km around NYC, is applied as a filter to select the storms that have return periods, in terms of the surge height at the Battery, greater than 10 yr, the typical range of hurricane surge periodicity relevant to design and policymaking. Second, the ADCIRC simulation, using an unstructured grid with a resolution of ~100 m around NYC (and up to 100 km over the deep ocean), is applied to each of the selected storms (see Supplementary Fig. S1, for a comparison between SLOSH and ADCIRC simulations). To determine whether the resolution of the ADCIRC simulation is sufficient, another ADCIRC mesh<sup>30</sup> with a resolution as high as ~10 m around NYC is used to simulate over 200 most extreme events under the observed climate condition. The differences between the results from the two grids are very small, with our ~100-m mesh overestimating the surge at the Battery by about 2.5% (Supplementary Fig. S2). Thus, the ~100-m ADCIRC simulations are used, with a 2.5% reduction of the surge magnitude, to estimate the surge levels at the Battery for return periods of 10 yr and longer. (ADCIRC model control parameters follow refs 29 and 30, whose results have been validated against observations.)

To quantify tide-surge nonlinearity, we generate a database of the storm surge and storm tide for over 200 most extreme events arriving every 3 h during a tidal cycle. We model the nonlinearity (denoted by  $L$ : the difference between simulated storm tide, surge and astronomical tide) as a function of the tidal phase ( $\varphi$ ) when the (peak) surge arrives, the surge height ( $H$ ), tidal range ( $t_r$ ) and mean tidal level ( $t_m$ ). We define a non-dimensional nonlinearity factor  $\gamma$  as

$$\gamma = \frac{L + t_m}{H + t_r} \tag{1}$$

so that, for a given value of  $\gamma$ , the higher the storm surge or the astronomical tide, the larger the nonlinearity relative to the negative mean tidal level ( $-t_m$ ; considering that the nonlinearity and the tide are out of phase; Supplementary Fig. S4). We use the generated storm surge and storm tide database to estimate  $\gamma$  by kernel regression as a function of the tidal phase (Supplementary Fig. S5). Then, the nonlinearity  $L$ , for a given tide and a surge corresponding to tidal phase  $\varphi$ , is estimated from equation (1) as

$$L(\varphi) = \gamma(\varphi)(H + t_r) - t_m \tag{2}$$

We assume the annual number of NY-region storms to be Poisson-distributed, with mean  $\lambda$ . The probability distribution of the surge height,  $P\{H < h\}$ , estimated from the generated surges for each storm set, is applied to estimate the PDF of the storm tide ( $H^t$ ),

$$P\{H^t < h\} = P\{H + t(\Phi) + L(\Phi) < h\} \tag{3}$$

where  $t$  is the height of the astronomical tide and  $\Phi$  is the (random) phase when the storm surge arrives. Making use of equation (2) and the estimated  $\gamma$  function,

equation (3) becomes

$$P\{H^t < h\} = \int_0^{2\pi} P\left\{H < \frac{h - t(\varphi) - \gamma(\varphi)t_r + t_m}{1 + \gamma(\varphi)}\right\} P\{\Phi = d\varphi\} \tag{4}$$

It is reasonable to assume that the surge can happen at any time during a tidal cycle with equal likelihood, and equation (4) becomes

$$P\{H^t < h\} = \int_0^{2\pi} P\left\{H < \frac{h - t(\varphi) - \gamma(\varphi)t_r + t_m}{1 + \gamma(\varphi)}\right\} \frac{1}{2\pi} d\varphi \tag{5}$$

(Note that equation (5) can be extended to include the effects of different tides during the hurricane season by taking a weighted average of  $P\{H^t < h\}$  for all types of tide considered, with weights equal to the fractions of time during the season when different types of tide occur.) Then, by definition, storm tide return period  $T^t$  is

$$T^t = \frac{1}{1 - e^{-\lambda(1 - P\{H^t < h\})}} \tag{6}$$

No analytical expression for the return level ( $h$ ) is available in this case; the storm tide return levels in Figs 2 and 3 are calculated by solving equations (5) and (6) numerically. The astronomical tide cycle observed at the site during the period of 18–19 September 1995 (NOAA tides and currents) is used, with an assumption that the tidal variation at NYC during the hurricane season is relatively small.

The surge PDF is also applied to estimate the PDF of the flood height ( $H^f$ ),

$$P\{H^f < h\} = P\{H + t(\Phi) + L(\Phi) + S < h\} \tag{7}$$

where  $S$  denotes the value of SLR, and the nonlinear effect of SLR on the surge is neglected. Then, on the basis of equation (5), equation (7) becomes

$$P\{H^f < h\} = \int_0^{s_m} \int_0^{2\pi} P\left\{H < \frac{h - t(\varphi) - \gamma(\varphi)t_r + t_m - s}{1 + \gamma(\varphi)}\right\} P\{S = ds\} \frac{1}{2\pi} d\varphi \tag{8}$$

where it is assumed that the range of possible SLR is  $[0, s_m]$ . The probability distribution of SLR may be estimated from GCM simulations and/or other methods<sup>21,47</sup>. It is also useful to estimate the flood return level for a certain SLR. For a given SLR ( $s$ ), equation (8) reduces to

$$P\{H^f < h\} = \int_0^{2\pi} P\left\{H < \frac{h - t(\varphi) - \gamma(\varphi)t_r + t_m - s}{1 + \gamma(\varphi)}\right\} \frac{1}{2\pi} d\varphi \tag{9}$$

The flood return period  $T^f$  is, similar to equation (6),

$$T^f = \frac{1}{1 - e^{-\lambda(1 - P\{H^f < h\})}} \tag{10}$$

The flood return levels in Fig. 4 are calculated by solving equations (9) and (10) numerically, assuming a SLR of 1 m ( $s = 1$ ) for the future climate (and  $s = 0$  for the present climate) and using the astronomical tide cycle observed during 18–19 September 1995. The statistical confidence interval of the estimated storm tide and surge flood return levels remains the same as the confidence interval of the estimated surge return level, as no new distribution parameters are introduced. The uncertainty in the estimation of the future return levels may be considered as the combination of the statistical confidence interval and the variation of predictions from different climate models.

Received 7 September 2011; accepted 2 January 2012; published online 14 February 2012

**References**

- Emanuel, K. The dependence of hurricane intensity on climate. *Nature* **326**, 483–485 (1987).
- Emanuel, K. The hurricane–climate connection. *Bull. Am. Meteorol. Soc.* **5**, ES10–ES20 (2008).
- Bender, M. A. *et al.* Model impact of anthropogenic warming on the frequency of intense Atlantic hurricanes. *Science* **327**, 454–458 (2010).
- Knutson, T. R. *et al.* Tropical cyclones and climate change. *Nature Geosci.* **3**, 157–163 (2010).
- Powell, M. D. & Reinhold, T. A. Tropical cyclone destructive potential by integrated kinetic energy. *Bull. Am. Meteorol. Soc.* **88**, 513–526 (2007).
- Resio, D. T. & Westerink, J. J. Hurricanes and the physics of surges. *Phys. Today* **61**, 33–38 (September 2008).
- Rego, J. L. & Li, C. On the importance of the forward speed of hurricanes in storm surge forecasting: A numerical study. *Geophys. Res. Lett.* **36**, L07609 (2009).
- Irish, J. L. & Resio, D. T. A hydrodynamics-based surge scale for hurricanes. *Ocean Eng.* **37**, 69–81 (2010).
- Irish, J. L., Resio, D. T. & Ratcliff, J. J. The Influence of storm size on hurricane surge. *J. Phys. Oceanogr.* **38**, 2003–2013 (2008).

10. Resio, D. T., Irish, J. L. & Cialone, M. A. A surge response function approach to coastal hazard assessment. Part 1: Basic concepts. *Nat. Hazard.* **51**, 163–182 (2009).
11. Irish, J. L., Cialone, M. A. & Resio, D. T. A surge response function approach to coastal hazard assessment. Part 2: Quantification of spatial attributes. *Nat. Hazard.* **51**, 83–205 (2009).
12. Knutson, T. R., Sirutis, J. J., Garner, S. T., Held, I. M. & Tuleya, R. E. Simulation of the recent multidecadal increase of Atlantic hurricane activity using an 18-km-grid regional model. *Bull. Am. Meteorol. Soc.* **88**, 1549–1565 (2007).
13. Knutson, T. R., Sirutis, J. J., Garner, S. T., Vecchi, G. A. & Held, I. M. Simulated reduction in Atlantic hurricane frequency under twenty-first-century warming conditions. *Nature Geosci.* **1**, 359–364 (2008).
14. Nicholls, R. J. Coastal megacities and climate change. *Geo. J.* **37**, 369–379 (1995).
15. Rosenzweig, C. & Solecki, W. Chapter 1: New York City adaptation in context. *Ann. NY Acad. Sci.* **1196**, 19–28 (2010).
16. Rosenzweig, C., Solecki, W., Hammer, S. A. & Mehrotra, S. Cities lead the way in climate-change action. *Nature* **467**, 909–911 (2010).
17. Emanuel, K., Ravela, S., Vivant, E. & Risi, C. A statistical deterministic approach to hurricane risk assessment. *Bull. Am. Meteorol. Soc.* **87**, 299–314 (2006).
18. Emanuel, K., Sundararajan, R. & Williams, J. Hurricanes and global warming: Results from downscaling IPCC AR4 simulations. *Bull. Am. Meteorol. Soc.* **89**, 347–367 (2008).
19. Emanuel, K., Oouchi, K., Satoh, M., Hirofumi, T. & Yamada, Y. Comparison of explicitly simulated and downscaled tropical cyclone activity in a high-resolution global climate model. *J. Adv. Model. Earth Sys.* **2**, 9 (2010).
20. Kalnay, E. *et al.* The NCEP/NCAR 40-year reanalysis project. *Bull. Am. Meteorol. Soc.* **77**, 437–471 (1996).
21. *IPCC Climate Change 2007: The Physical Science Basis* (eds Solomon, S. *et al.*) (Cambridge Univ. Press, 2007).
22. Jarvinen, B. R., Neumann, C. J. & Davis, M. A. S. *A Tropical Cyclone Data Tape for the North Atlantic Basin, 1886–1983: Contents, Limitations, and Uses* NOAA Tech. Memo NWS NHC 22 (NOAA/Tropical Prediction Center, 1984).
23. Villarini, G., Vecchi, G. A., Knutson, T. R., Zhao, M. & Smith, J. A. North Atlantic tropical storm frequency response to anthropogenic forcing: Projections and sources of uncertainty. *J. Clim.* **24**, 3224–3238 (2011).
24. Luettich, R. A., Westerink, J. J. & Scheffner, N. W. *ADCIRC: An Advanced Three-dimensional Circulation Model for Shelves, Coasts and Estuaries, Report 1: Theory and Methodology of ADCIRC-2DDI and ADCIRC-3DL* DRP Technical Report DRP-92-6. (Department of the Army, US Army Corps of Engineers, Waterways Experiment Station, 1992).
25. Westerink, J. J., Luettich, R. A., Blain, C. A. & Scheffner, N. W. *ADCIRC: An Advanced Three-Dimensional Circulation Model for Shelves, Coasts and Estuaries; Report 2: Users Manual for ADCIRC-2DDI* (Department of the Army, US Army Corps of Engineers, 1994).
26. Jelesnianski, C. P., Chen, J. & Shaffer, W. A. *SLOSH: Sea, Lake, and Overland Surges from Hurricanes* (NOAA Tech. Report NWS 48, 1992).
27. Jarvinen, B. R. & Lawrence, M. B. Evaluation of the SLOSH storm-surge model. *Bull. Am. Meteorol. Soc.* **66**, 1408–1411 (1985).
28. Jarvinen, B. & Gebert, J. *Comparison of Observed versus SLOSH Model Computed Storm Surge Hydrographs along the Delaware and New Jersey Shorelines for Hurricane Gloria, September 1985* (US Department of Commerce, National Hurricane Center, 1986).
29. Westerink, J. J. *et al.* A basin- to channel-scale unstructured grid hurricane storm surge model applied to southern Louisiana. *Mon. Weath. Rev.* **136**, 833–864 (2008).
30. Colle, B. A. *et al.* New York City's vulnerability to coastal flooding. *Bull. Am. Meteorol. Soc.* **89**, 829–841 (2008).
31. Lin, N., Smith, J. A., Villarini, G., Marchok, T. P. & Baek, M. L. Modeling extreme rainfall, winds, and surge from Hurricane Isabel (2003). *Weath. Forecasting* **25**, 1342–1361 (2010).
32. Dietrich, J. C. *et al.* Modeling hurricane waves and storm surge using integrally-coupled, scalable computations. *Coast. Eng.* **58**, 45–65 (2011).
33. Emanuel, K. & Rotunno, R. Self-stratification of tropical cyclone outflow. Part I: Implications for storm structure. *J. Atmos. Sci.* **68**, 2236–2249 (2011).
34. Georgiou, P. N., Davenport, A. G. & Vickery, B. J. Design windspeeds in regions dominated by tropical cyclones. *J. Wind Eng. Ind. Aerodyn.* **13**, 139–159 (1983).
35. Bretschneider, C. L. *A Non-dimensional Stationary Hurricane Wave Model* Vol. I, 51–68 (Proc. Offshore Technology Conference, 1972).
36. Holland, G. J. An analytic model of the wind and pressure profiles in hurricanes. *Mon. Weath. Rev.* **108**, 1212–1218 (1980).
37. Scileppi, E. & Donnelly, J. P. Sedimentary evidence of hurricane strikes in western Long Island, New York. *Geochem. Geophys. Geosyst.* **8**, 1–25 (2007).
38. Coles, S. *An Introduction to Statistical Modelling of Extreme Values* (Springer, 2001).
39. Lin, N., Emanuel, K. A., Smith, J. A. & Vanmarcke, E. Risk assessment of hurricane storm surge for New York City. *J. Geophys. Res.* **115**, D18121 (2011).
40. Horton, R. M. *et al.* Climate hazard assessment for stakeholder adaptation planning in New York City. *J. Appl. Meteorol. Climatol.* **50**, 2247–2266 (2011).
41. Colle, B. A., Rojowsky, K. & Buonaiuto, F. New York City storm surges: Climatology and analysis of the wind and cyclone evolution. *J. Appl. Meteorol. Climatol.* **49**, 85–100 (2010).
42. Chavas, D. R. & Emanuel, K. A. A QuikSCAT climatology of tropical cyclone size. *Geophys. Res. Lett.* **37**, L18816 (2010).
43. Emanuel, K. A. An air–sea interaction theory for tropical cyclones. Part I: Steady-state maintenance. *J. Atmos. Sci.* **43**, 585–605 (1986).
44. Emanuel, K. Environmental factors affecting tropical cyclone power dissipation. *J. Clim.* **20**, 5497–5509 (2007).
45. Gornitz, V., Couch, S. & Hartig, E. K. Impacts of sea level rise in the New York City metropolitan area. *Glob. Planet. Change* **32**, 61–88 (2001).
46. Yin, J., Schlesinger, M. E. & Stouffer, R. J. Model projections of rapid sea-level rise on the northeast coast of the United States. *Nature Geosci.* **2**, 262–266 (2009).
47. Horton, R., Gornitz, V. & Bowman, M. Chapter 3: Climate observations and projections. *Ann. NY Acad. Sci.* **1196**, 41–62 (2010).
48. Hunter, J. Estimating sea-level extremes under conditions of uncertain sea-level rise. *Climatic Change* **99**, 331–350 (2010).
49. Mousavi, M. E., Irish, J. L., Frey, A. E., Olivera, F. & Edge, B. L. Global warming and hurricanes: The potential impact of hurricane intensification and sea level rise on coastal flooding. *Climatic Change* **104**, 575–597 (2010).
50. Hoffman, R. N. *et al.* An estimate of increases in storm surge risk to property from sea level rise in the first half of the twenty-first century. *Weath. Clim. Soc.* **2**, 271–293 (2010).

## Acknowledgements

N.L. was supported by the National Oceanic and Atmospheric Administration Climate and Global Change Postdoctoral Fellowship Program, administered by the University Corporation for Atmospheric Research, and the Princeton Environmental Institute and the Woodrow Wilson School of Public and International Affairs for the Science, Technology and Environmental Policy fellowship. We acknowledge the National Science Foundation and the National Center for Atmospheric Research's Computational and Information Systems Laboratory computational support. We thank J. Westerink and S. Tanaka of the University of Notre Dame for their support on the ADCIRC implementation. We also thank B. Colle of Stony Brook University for providing us with the high-resolution ADCIRC mesh.

## Author contributions

All authors contributed extensively to the work presented in this paper, and all contributed to the writing, with N.L. being the lead author.

## Additional information

The authors declare no competing financial interests. However, in the interests of transparency we confirm that one of us, Kerry Emanuel, is on the boards of two property and casualty companies: Homesite and Bunker Hill, and also on the board of the AlphaCat Fund, an investment fund dealing with re-insurance transactions. In all three cases, Dr Emanuel receives fixed fees but owns no stocks or shares. Dr Emanuel does not stand to make any personal financial gain through these directorships as a consequence of the reported findings.

Supplementary information accompanies this paper on [www.nature.com/natureclimatechange](http://www.nature.com/natureclimatechange). Reprints and permissions information is available online at [www.nature.com/reprints](http://www.nature.com/reprints). Correspondence and requests for materials should be addressed to N.L.